https://doi.org/10.61308/TAGD6115

Possibilities of small robotic UAVS for surveillance of agricultural areas in Southern Dobruja

Asparuh Atanasov*
dept. Mechanics and Elements of Machines, Technical University of Varna, Varna, Bulgaria
ORCID: 0000-0001-9898-8472
*E-mail: *asparuh.atanasov@tu-varna.bg*

Citation: Atanasov, A. (2024). Possibilities of small robotic UAVS for surveillance of agricultural areas in Southern Dobruja. *Bulgarian Journal of Crop Science, 61*(3) 100-108

Abstract: Timely diagnosis of trends in the development of agricultural crops is essential for precision agriculture. The use of unmanned aerial vehicles (UAV) allows us to quickly and accurately collect information about crops. The study tests the capabilities of a small aircraft in the fields of Dobruja, Bulgaria. We tested two small aircrafts with their built-in cameras and a near-infrared camera. An early diagnosis of a reduced vegetation index due to pathogens and a defect in the planter was confirmed. The obtained dependencies show the possibility of using aircraft in the agrometeorological situation of Dobruja.

Keywords: UAV; precision agriculture; vegetation indices; NDVI

INTRODUCTION

Every time we look at an object, we see light of specific colors reflected back to us. We perceive only what our eyes can perceive. When looking at plants, we will usually see a predominance of green. Green light is reflected by plants because they don't use it when they absorb energy from the sun.

Photogrammetry includes all techniques involved in making measurements of real-world objects and terrain features from images (James et al., 2010). Use of radiometry in photogrammetry, using specific sensors and cameras that capture near-infrared light. Data from these cameras can be used for agricultural photogrammetry. Through specialized formulas, we can create vegetation index. This is a 2D map of a crop or field, that analyzes how plants reflect light (Mejia-Zuluaga et al., 2021).

The application of photogrammetry in agriculture is by measuring the reflected light in the different spectral regions and comparing them. Various reflective vegetation indices have been created for this purpose. The most popular is NDVI - normalized difference vegetation index (Rouse et al., 1974). It characterizes the density of the vegetation, the stage of growth, the presence of weeds or diseases, it is used to predict yields. The indices are generated by taking pictures of green vegetation that absorbs electromagnetic waves in the visible red range and reflects them in the near infrared range. The red region of the spectrum (0.66 µm) accounts for the maximum absorption of solar radiation by chlorophyll, and the reflection of near-infrared light (0.85 µm). Its formula is:

$$\text{NDVI} = \frac{R_n - R_r}{R_n + R_r} \quad (1)$$

Where: Rn is the infrared spectrum of light, Rr is the red spectrum of light.

VARI - Visible Atmospherically Resistant Index (Gitelson et al., 2002). It is minimally sensitive to atmospheric influences; this allows the vegetation to be assessed accurately. This vegetation index is based on RGB and takes into account the presence of blue when calculating the spectral data. Its formula is:

$$\text{VARI} = \frac{R_g - R_r}{R_g + R_r - R_b} \quad (2)$$

Where: Rg is the green light spectrum, Rr is the red light spectrum, Rb is the blue light spectrum.

Yield prediction and plant health verification are traditionally determined by representative sampling with manual sampling (Pothen & Nuske, 2016). Yield estimation with visual inspection by counting spikes, plants and size estimation is subjective, leading to errors in the differences between different results, among different observers according to their experience (Roscher et al., 2014). The presence of mud very high or low temperatures make sampling difficult. Advances in technology allow the assessment to be carried out by aircraft (Atanasov et al., 2023). There are more and more cameras with RGB and NIR spectrum that can be mounted on a drone and by means of which reflective vegetation indices can be obtained (Scotford et al., 2005).

The research aims to establish the applicability of remote spectral methods using a drone for the assessment of agricultural crops in the region of southern Dobruja. For this purpose, the possibilities of UAVs in researching small and agricultural areas during flights under the cloud cover at a low flight height of up to 100m above the terrain are being investigated. Establishing the influence of the specific agrarian climatic features of the region on the possibility of observation. Purpose of this article is to research the possibilities of types of cameras and the dynamics of the obtained results.

MATERIAL AND METHODS

The study includes two small UAVs tested and the argoclimatic features of southern Dobruja, Bulgaria. The climate in the district is characterized by cold winters and hot summers. The area is characterized by almost constant winds, which at times reach up to 20 m/s. Their possibilities for the assessment of agricultural crops by means of remote spectral sensing have been investigated. The tested drones are shown in Figure 1. They are used UAV DJI Mavic 2 pro and DJI Phan-

a) b)

Figure 1. UAVs DJI Mavic 2 pro (a) and DJI Phantom 4 Pro+ (b)

Table 1. Main characteristics of the UAVs used (Dji, 2023)

Parameter \ Dron	MAVIC 2 PRO	PHANTOM 4 PRO+
Weight	907g	1388g
Max Flight Time	31 min	30 min
Flight altitude above the terrain	120 m	500 m
Max Speed	72 km/h	72 km/h
Max Wind Speed Resistance	8 m / s	10 m / s
Operating Temperature Range	-10°C to 40°C	0° to 40°C
Transmission Distance (Unobstructed, free of interference)	FCC: 10 km	FCC: 7 km

tom 4 Pro+ (Dji, 2023), data on them are given in Table 1.

The cameras used in the study and their main parameters are listed in Table 2 and shown in Figure 2. Both cameras are built into the aircraft used. The drone is also equipped with a MAPIR Survey3 camera (Mapir, 2023), which takes pictures independently of the carrier.

According to the manufacturer's specification, the maximum flight time is 31 min (without wind and speed 25 km/h) [dji.com, 2023]. It is known that it is possible to use the maximum flight height of the UAV of 120 m. The theoretical flight time does not correspond to the actual flight situation due to the variable values of wind, humidity and air temperature. Equipping the drone with an additional camera also disrupts aerodynamics, increases weight and decreases flight time. This changes the size of the plot that can be flown over. Consequently, the set plot size and the planned flight time must be considered.

During the flights conducted, it was found that after the UAV's battery drops to 25%, it begins to issue a low charge warning signal, and after falling below 10%, it goes into a controlled landing at the coordinates it is on. The optimal flight time in scan mode was found to be about 20 minutes.

The size of the scanned area depends on the horizontal speed of the UAV for the specific model. In the conducted UAV tests, it varies from 8 to 11 m/s in "P" mode when scanning. The size of the field that can be flown over also depends on the overlapping of the pictures, which can be chosen to be 70, 80 or 90%. The resolution of the camera sensor also affects the size of the scanned area.

The shooting is carried out along a meander trajectory relative to the flight height and the selected photo overlap relative to the size of the sensor matrix. The capabilities of two software products for capturing agricultural areas are tested. Shown in Figure 3a is the DroneDeploy window (DroneDeploy, 2023) and in Figure 3b PIX4Dcapture (PIX4Dcapture, 2023).

Determining the size of one pixel of the resulting image to how many meters of the field corresponds to a series of flights over an area of 100 x 100 m at different altitudes with a planned overlap of 80%. When flying at a height lower than 20 meters, there is a danger of collision with the field protection plants. For this reason, tests have been carried out at a height of 20 to 100m (this is the maximum permitted height for the flight of a small UAV). The planned flight for the DJI

Table 2. Types of cameras used in the study

Hasselblad c 20MP 1" CMOS	Sony Exmor R IMX117 12MP	DJI FC6310 8.8
Red+Green+Blue (RGB)	Red+Green+NIR (RGN)	Red+Green+Blue (RGB)
Resolution 20MP	Resolution 12MP	Resolution 20MP
Photo 5472×3648	Photo 4000x3000	Photo 5472x3648
Lens FOV 77°, 28 mm	Lens 41° HFOV, 47mm	Lens FOV 84° 8.8 mm/24 mm

a) b) c)

Figure 2. Cameras: Hasselblad (a) [Dji, 2023], Sony Exmor R [Mapir, 2023] (b) and DJI FC6310 (c) [Dji, 2023]

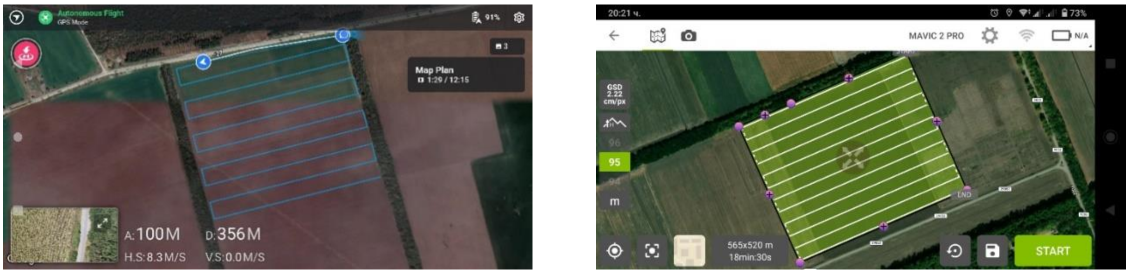

a) b)

Figure 3. Software DroneDeploy (a) and PIX4Dcapture (b)

Table 3. Parameters of the planned flight

	20 m	**30 m**	**40 m**	**50 m**	**60 m**	**70 m**	**80 m**	**90 m**	**100 m**
GSD cm/px	0,47	0,7	0,94	1,17	1,41	1,64	1,87	2,11	2.34
Flight time (min)	17	10	7:30	6:30	6	5:30	5:30	5:30	6
Number of meanders	14	10	8	7	6	5	5	4	4

Mavic 2 pro and its data are shown in Table 3. Flight time increases at higher altitudes because the time for takeoff (reaching the set altitude) and landing increases.

Flight planning is based on weather conditions and restricted areas. Flights at temperatures below 5°C are not conducted due to the risk of propeller icing. At this temperature, the plants are at rest and there are no changes in the vegetation indices.

RESULTS AND DISCUSSION

After the irrigation of an experimental trial field, the obtained results are shown in Table. 4 for the period 05. 04. 2022 – 05. 07. 2022 г.

During the period of the flight, the maximum wind speed was 8 m/s, which does not exceed the characteristics of the UAV and does not hinder the flight.

The testing of the ratio of the flight height above the terrain and the size of the sensor matrix to the size of the terrain obtained in one pixel is shown in Table 5. With information from a satellite, the approximate size of 1 pixel is about a square meter, and the values obtained even at a height of 120 m are 3-4 cm.

The main limitation of the flight is the loss of energy in the battery. The main limiting factor besides energy is wind. Which in the area is often moderate to strong. This necessitates testing the maximum possible area that can be flown. Flight planning allows the length and width overlap to vary from 70-90%. As the percentage decreases, the coverage area increases. During tests, it was found (Figure 4) that the maximum area at 70% overlap and 100m height at a set flight speed of 10 m/s is 800x700 m - 0.56 km^2. At 90% overlap it is approx 0,35 km^2.

The conducted flights confirmed that wind up to 8 m/s does not affect the filming of agricultural areas. With the DJI Phantom 4 Pro, filming is possible up to a wind speed of 11.5 m/s.

When planning three flight areas with common sides and simultaneous processing of information, data was obtained for an area of 1.25 km^2, the plan is shown in Figure 5. Flight time – 43 min. Obtaining a detailed map of the vegetation of the observed area saves time for the specialist as well and gives detailed information and not a representative sample, as in sampling.

Table 4. conducted flights against the background of climatic features

Date	**5.4. 2022**	**26.4. 2022**	**3.5. 2022**	**10.5. 2022**	**17.5. 2022**	**25.5. 2022**	**31.5. 2022**	**7.6. 2022**	**21.6. 2022**	**28.6. 2022**	**5.7. 2022**
Humidity (%)	76	77	72	52	68	83	54	83	61	48	42
Cloudiness (%)	19	45	97	21	20	13	44	90	18	56	10
Temperature at capture (C)	8	17	13	17	20	17	27	19	24	28	27
E - lighting (lx)	98010	46940	21860	61340	100080	107790	108830	123060	108890	128050	103740
CCT (K)	6013	6631	6434	6179	5877	6101	5950	5941	5900	5728	5858
Wind speed (m/s)	2	1	2	2	3	3	3	6	4	8	1
Wind direction	North-east	North-east	Nort	South	South	East	North West	Nort	South	Nort	East
Area	532x 538	532x 538	532x 538	532x 538	532x 538	532x 538	532x 538	532x 538	532x 538	532x 538	532x 538
Flight time	10min: 30s	10min: 30s	10min: 30s	10min: 30s	10min: 30s	10min: 30s	10min: 30s	10min: 30s	10min: 30s	10min: 30s	10min: 30s
Altitude (m)	100	100	100	100	100	100	100	100	100	100	100
UAV	Mavic 2 pro	Mavic 2 pro	Mavic 2 pro	Mavic 2 pro	Mavic 2 pro	Mavic 2 pro	Mavic 2 pro	Mavic 2 pro	Mavic 2 pro	Mavic 2 pro	Mavic 2 pro
Number of photos	93	107	128	335	100	101	108	101	126	105	97
Ground Sampling Distance - GSD (sm/px)	2,34	2,34	2,34	2,34	2,34	2,34	2,34	2,34	2,34	2,34	2,34
Average GSD (sm/px)	2,25	2,22	2,45	2,44	2,35	2,39	2,36	2,03	2,35	2,28	2,33
NDVI max	0,23	0,27	0,36	0,36	0,34	0,16	0,31	0,32	0,10	0,11	0,09

Table 5. Pixel size according to shooting height and sensor type

sensor MAPIR Survey 3W	**sensor Hasseblad L1D-20c**
Altitude 20 m - 0.77 cm / px	Altitude 20 m - 0.47 cm / px
Altitude 40 m - 1.56 cm / px	Altitude 40 m - 0.94 cm / px
Altitude 60 m - 2.48 cm / px	Altitude 60 m - 1.41 cm / px
Altitude 80 m - 3.18 cm / px	Altitude 80 m - 1.55 cm / px
Altitude 100 m - 4.09 cm / px	Altitude 100 m - 2.34 cm / px
Altitude 120 m* - 4.37 cm / px	Altitude 120 m* - 3.10 cm / px

* - *maximum permitted flight altitude.*

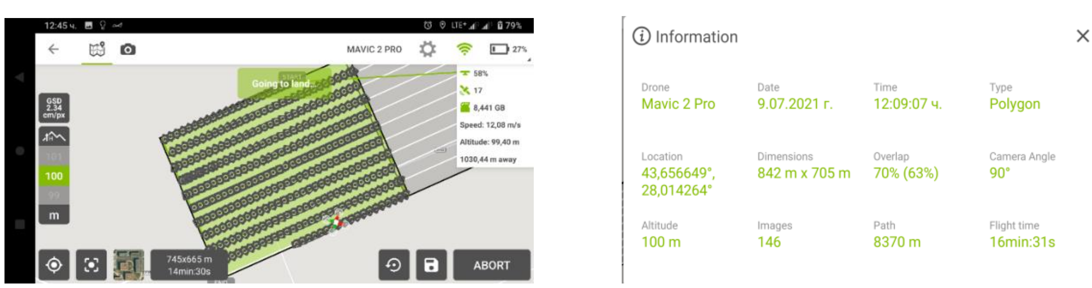

a) b)

Figure 4. Flight report (a) and flight information (b)

A picture of the field in the visible spectrum RGB, with the near infrared light RNG and the generated NDVI index on 06/05/2021 are shown on Figure 6. It can be seen that there is no visual problem in the two photos, but the generated vegetation index shows an area with reduced vegetation. The change in near-infrared reflectance is known to occur 10 days before the change in visible light. This allows for early diagnosis before a person's eye registers the change.

The diagnosis of the appearance of yellow rust is shown on Figure 7. On the figure, the area is indicated with an arrow. As a result of the obtained spots on the map, on 24.05.2021 it was checked on site and the appearance of yellow blight was confirmed, with its growth, an increase in the spot with reduced vegetation on the map is visible until it covers the entire crop.

Diagnosis of an area with reduced NDVI on an experimental wheat field 2021-2022 indicated by an arrow. Due to the later processing of the results, the reason for the reduced vegetation index has not been confirmed. Fig.8 shows the appearance of a zone with lower NDVI that grows in the following days. The zone is sown with one variety of wheat and is initially of the same shade.

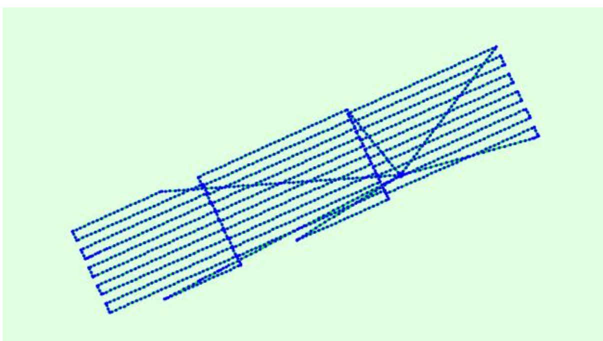

Figure 5. Plan with overlapping flight areas. The take-off point is visible.

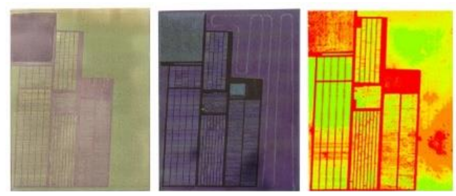

Figure 6. Photo of experimental field in RGB, RGN and NDVI index

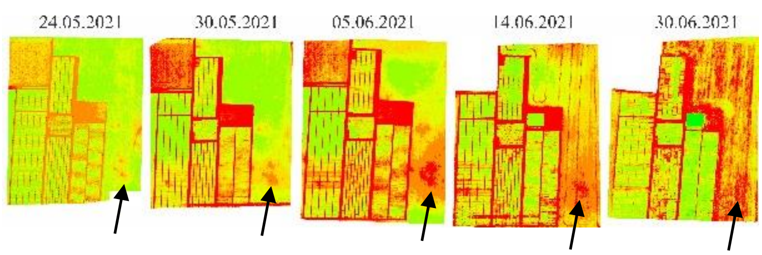

Figure 7. NDVI map of the experimental field with the period of occurrence of yellow rust

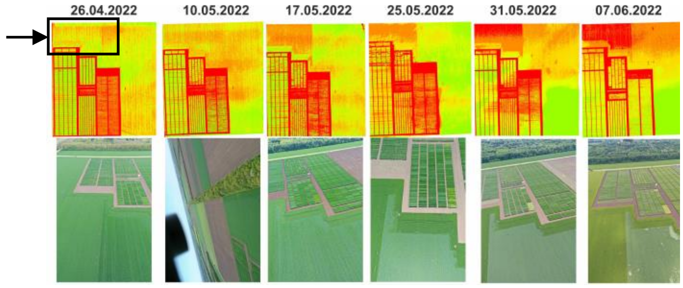

Figure 8. NDVI map of the experimental field and RGB photo of the low-index sonar

As NDVI decreases, the color in the visible spectrum changes.

Figure 9 shows the NDVI of the experimental field during the period 2020-2022. It can be traced that the areas with reduced vegetation do not exist in an earlier stage of development. It follows that the presence of pathogens is diagnosed. The methodology can be used as an auxiliary tool, but it cannot replace the agronomist. Surveying the area using a small aerial vehicle is quick and can save time in the diagnostic stage.

Figure 10 presents the comparison of NDVI and VARI vegetation index. The first one was obtained from the MAPIR camera and the second one from the drone's built-in camera, which shoot independently of each other.

A comparison of the two vegetation indices shows nearly identical maps for areas with low

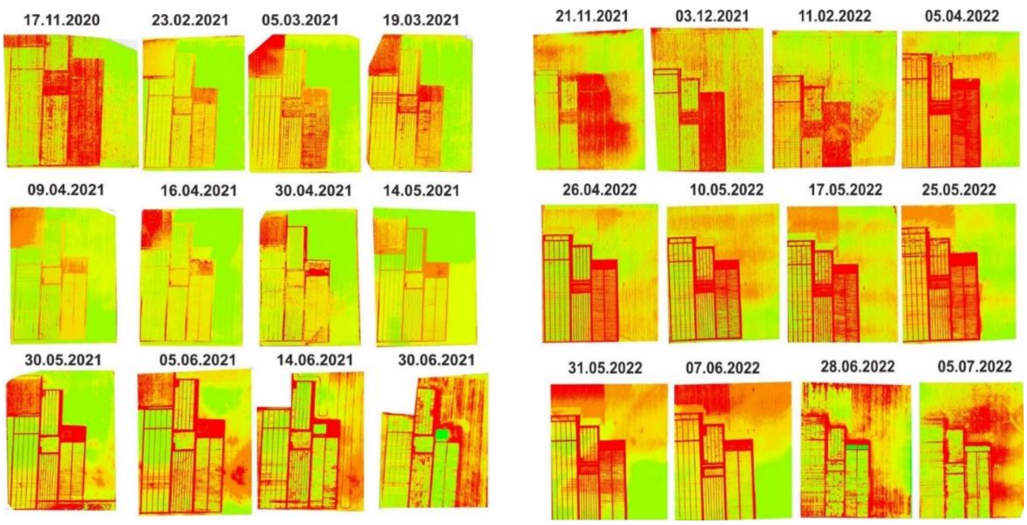

a) b)

Figure 9. NDVI experimental wheat field 2020-2021(a), 2021-2022(b)

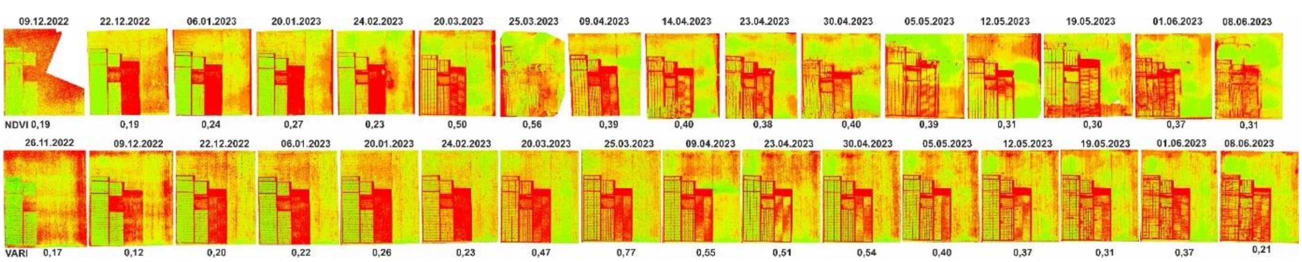

Figure 10. NDVI and VARI experimental wheat field 2022-2023

a) b) c)

Figure 11. NDVI in a field of wheat - 17.05.2022 (a), RGB photo at eye level (b) and RGB photo from 100m height (c)

and high vegetation. This gives us the opportunity, in the absence of a near-infrared camera, to use the built-in RGB camera in the drone.

The possibility of diagnosing improperly planned agrotechnical measures or problems with agricultural machinery was confirmed when observing a field with wheat Figure 11. Figure 11a shows the NDVI map of the field with alternating areas of low and high vegetation. Figure 11b shows an RGB photograph of the field from a shooting height of 1.7 m. Figure 11c shows an RGB photo taken by the drone from a height of 100m. Areas of different color are visible. During on-site visits, it was diagnosed that the crop was developing normally, but with low coverage. After consultation with the farmer, it was established that this was due to a problem in the seeder. One section did not release evenly, therefore the sowing is thinned out and part of the soil is also visible when photographed vertically.

The general trend of changes in the vegetation index NDVI for the field is shown on Figure 12. It can be seen that the alternation of areas with low and high vegetation is throughout the period.

Conducted research flights over a period of 3 business years are 246, which is ≈120 flight hours.

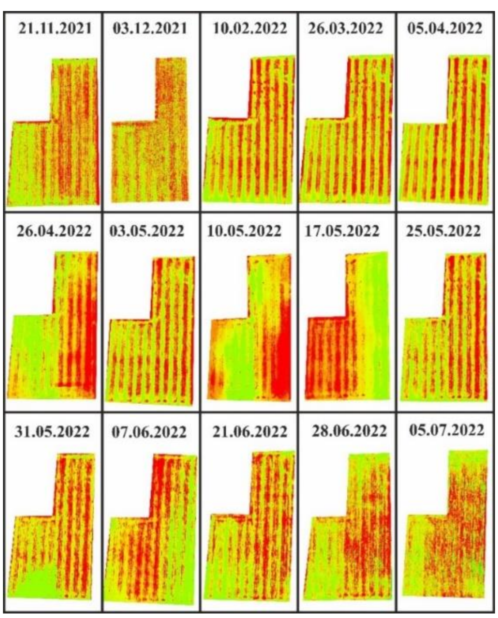

Figure 12. NDVI of a wheat field 2021-2022 with alternating areas of low and high vegetation

During this time, wear and tear in the UAV was not detected (Bankova, 2022)

CONCLUSIONS

As a result of the experiments carried out in the region of southern Dobruja, the possibility of monitoring agricultural areas by means of a small aerial vehicle has been confirmed. The agrometeorological features of the area do not affect the possibility of flooding the areas. Strong winds that would impede flights are very rare and can be avoided with planning.

The obtained results show the possibilities of the method for early diagnosis of the appearance of pathogens by means of research in the NIR spectrum. The ability to diagnose using the drone's built-in RGB camera has also been confirmed. They can facilitate the agronomist in his work by providing him with quick and accurate information about the zones of different vegetation in the field.

The methodology also proves the effectiveness of diagnosing certain problems when carrying out the planned agrotechnical measures. This would allow us to diagnose problems and eliminate deficiencies.

The methodology is suitable for small and ultra-small areas where it is impossible to obtain data on trends in changes in reflective vegetation indices. It is applicable for carrying out tests during selection activity.

REFERENCES

Atanasov, A., Bankova, A., & Zhecheva, G. (2023). Result Processing Methodology for the Vegetation Processes Remote Sensing by a Small Unmanned Aerial Vehicle, *Bulgarian Journal of Agricultural Science, 29* (3), 564–569, https://agrojournal.org/29/03-22.html

Bankova, A. (2022). "Investigation of the Qualitative Dependence between the Character of Wear and the Mutual Location of Wearing Supports," 2022 International Conference on Communications, Information, Electronic and Energy Systems (CIEES), Veliko Tarnovo, Bulgaria, 2022, pp. 1-4, doi: 10.1109/CIEES55704.2022.9990870.

Gitelson, A. A., Kaufman, Y. J., Stark, R., & Rundquist, D. (2002). Novel algorithms for remote estimation of vegetation fraction. *Remote sensing of Environment*, *80*(1), 76-87.

Dji. (2023). https://www.dji.com/

DroneDeploy. (2023). https://www.dronedeploy.com/

Aber, J. S., Marzolff, I., & Ries, J. B. (2010). Chapter 3-photogrammetry. *Small-Format Aerial Photography*, 23-39. ISBN 9780444532602. https://doi.org/10.1016/B978-0-444-53260-2.10003-1

Mejia-Zuluaga, P. A., Dozal-García, L. F., & Valdiviezo-Navarro, J. C. (2021). Detection of Phoradendron Velutinum Implementing Genetic Programming in Multispectral Aerial Images in Mexico City. In *International Conference on Geospatial Information Sciences* (pp. 109-129). Cham: Springer International Publishing. https://doi.org/10.1007/978-3-030-98096-2_9

Mapir. (2023). https://www.mapir.camera/collections/survey3

PIX4Dcapture. (2023). https://www.pix4d.com/

Pothen, Z., & Nuske, S. (2016). Automated assessment and mapping of grape quality through image-based color analysis. *IFAC-PapersOnLine*, *49*(16), 72-78.

Roscher, R., Herzog, K., Kunkel, A., Kicherer, A., Töpfer, R., & Förstner, W. (2014). Automated image analysis framework for high-throughput determination of grapevine berry sizes using conditional random fields. *Computers and Electronics in Agriculture*, *100*, 148-158.

Rouse, J. W., Haas, R. H., Schell, J. A., Deering, D. W., & Harlan, J. C. (1974). Monitoring the vernal advancement of retrogradation of natural vegetation (p. 371). Greenbelt, MD: NASA/GSFC (Type III, Final Report).

Scotford, I. M., & Miller, P. C. H. (2005). Applications of spectral reflectance techniques in northern European cereal production: a review. *Biosystems engineering*, *90*(3), 235-250. https://doi.org/10.1016/j.biosystemseng.2004.11.010.

Received: December 21 2023; *Approved:* May 12 2024; *Published:* June 2024